JOURNAL OF GENERAL VIROLOGY

RESEARCH ARTICLE

Muth *et al.*, *Journal of General Virology* 2017;98:2461–2469

DOI 10.1099/jgv.0.000919

MICROBIOLOGY SOCIETY

Transgene expression in the genome of Middle East respiratory syndrome coronavirus based on a novel reverse genetics system utilizing Red-mediated recombination cloning

Doreen Muth,[1,2,3]† Benjamin Meyer,[2]† Daniela Niemeyer,[1,2] Simon Schroeder,[1,2] Nikolaus Osterrieder,[4] Marcel Alexander Müller[1,2] and Christian Drosten[1,2,3,*]

Abstract

Middle East respiratory syndrome coronavirus (MERS-CoV) is a high-priority pathogen in pandemic preparedness research. Reverse genetics systems are a valuable tool to study viral replication and pathogenesis, design attenuated vaccines and create defined viral assay systems for applications such as antiviral screening. Here we present a novel reverse genetics system for MERS-CoV that involves maintenance of the full-length viral genome as a cDNA copy inserted in a bacterial artificial chromosome amenable to manipulation by homologue recombination, based on the bacteriophage λ Red recombination system. Based on a full-length infectious MERS-CoV cDNA clone, optimal genomic insertion sites and expression strategies for GFP were identified and used to generate a reporter MERS-CoV expressing GFP in addition to the complete set of viral proteins. GFP was genetically fused to the N-terminal part of protein 4a, from which it is released during translation via porcine teschovirus 2A peptide activity. The resulting reporter virus achieved titres nearly identical to the wild-type virus 48 h after infection of Vero cells at m.o.i. 0.001 (1×10^5 p.f.u. ml^{-1} and 3×10^5 p.f.u. ml^{-1}, respectively), and allowed determination of the 50 % inhibitory concentration for the known MERS-CoV inhibitor cyclosporine A based on fluorescence readout. The resulting value was 2.41 μM, which corresponds to values based on wild-type virus. The reverse genetics system described herein can be efficiently mutated by Red-mediated recombination. The GFP-expressing reporter virus contains the full set of MERS-CoV proteins and achieves wild-type titres in cell culture.

INTRODUCTION

Middle East respiratory syndrome coronavirus (MERS-CoV) has been identified by the World Health Organization (WHO) as one of the priority pathogens to be studied in the context of outbreak preparedness and intervention [1]. As of 24 April 2017, 1936 cases of MERS-CoV infection have been reported, including 690 (35.6 %) deaths [2]. MERS-CoV poses a serious and continuing threat to international public health because of its source in a livestock species and its transmission route via the respiratory tract [3, 4]. Dromedary camels show high seropositivity, in the range 55–95 %, depending on age [5]. Between 25 and 59 % of camels may actively shed the virus, providing an opportunity for frequent animal-to-human transmission in vulnerable persons [5, 6]. Serological evidence suggests that MERS-CoV in camels must have been enzootic in East Africa and the Middle East for several decades [5, 7, 8]. Although human-to-human transmissibility of MERS-CoV is generally low, introduction into health care settings can lead to virus amplification and limited onward transmission [9–11]. Hospital-associated mortality can range between 14.5 and 65 % [12–14]. Currently, there is no approved vaccine and only limited clinical data on disease outcome under empirical treatments such as interferon (IFN), ribavirin or corticosteroids (both reviewed in [15, 16]). The reasons for the high pathogenicity associated with MERS-CoV in comparison to other CoVs remain to be determined.

Received 16 May 2017; Accepted 13 August 2017

Author affiliations: [1]Institute of Virology, Helmut-Ruska-Haus, Charité - Universitätsmedizin Berlin, Charitéplatz 1, 10117 Berlin, Germany; [2]Institute of Virology, University of Bonn Medical Centre, Sigmund-Freud-Str. 25, 53127 Bonn, Germany; [3]German Centre for Infection Research (DZIF), Inhoffenstraße 7, 38124 Braunschweig, Germany; [4]Institut für Virologie, Robert von Ostertag-Haus, Zentrum für Infektionsmedizin, Freie Universität Berlin, Robert-von-Ostertag-Str. 7-13, 14163 Berlin, Germany.

***Correspondence:** Christian Drosten, christian.drosten@charite.de

Keywords: MERS-CoV; reverse genetics; recombination; reporter virus.

Abbreviations: BAC, bacterial artificial chromosome; BHK, baby hamster kidney; CsA, cyclosporin A; IFN, interferon; MERS-CoV, Middle East respiratory syndrome coronavirus; SARS-CoV, severe acute respiratory syndrome coronavirus; TRS, transcription-regulatory sequence; WHO, World Health Organization.

†These authors contributed equally to this work.

Pathogenicity and interference with the host defences in CoV may be influenced by accessory proteins enconded in the viral genome. Among the MERS-CoV accessory proteins, 4a (p4a), p4b and p5 were studied for their IFN antagonistic properties. P4a was found to inhibit the IFN induction pathway by suppressing dsRNA-mediated infection sensing. Another important component of p4a activity is interference with PKR-mediated stress response [17, 18]. MERS-CoV p4b has phosphodiesterase activity and counteracts the IFN response by antagonizing activation of the 2′, 5′-oligoadenylate synthetase/RNase L pathway [19]. Other studies have identified activities against IFN beta expression [20, 21]. P5 inhibits the induction of IFN-β production by preventing nuclear translocation of IFN regulatory factor 3 [22]. Reverse genetics is a valuable tool to modify and study the function of viral proteins in the context of a replicating virus.

Coronavirus reverse genetics is challenging because of the difficulty in stably cloning large and continuous viral genes in bacteria. Based on prior experience with SARS-CoV [23], we present a novel reverse genetics system for MERS-CoV that combines advantageous features of several classical approaches in coronavirus reverse genetics. It relies on T7-based *in vitro* RNA transcription to avoid the risk of unwanted splicing of long virus RNA genomes in the cell. The full-length genome is propagated in an *E. coli* bacterial artificial chromosome (BAC) plasmid to circumvent *in vitro* ligation steps and provide a high yield of cDNA template. To enable more efficient mutagenesis on full-length BAC-contained viral cDNA, we introduced two-step Red-mediated recombination mutagenesis [24]. Application of the technique is demonstrated by the generation of different variants of MERS-CoV reporter-expressing viruses.

RESULTS

Based on the existing reverse genetics system for SARS-CoV, a new system for MERS-CoV was established. Six subgenomic fragments were reverse transcribed from viral RNA into cDNA, amplified by PCR and cloned into BAC vector pBeloBAC via primer-added restriction sites. Stepwise assembly of the full-length genome was achieved using naturally occurring restriction sites as shown in (Fig. 1a). An SwaI restriction site at genome position 20 764 was deleted while maintaining the amino acid sequence to enable subsequent cloning steps. This silent mutation also served as a marker mutation to distinguish wild-type from recombinant MERS-CoV (rMERS-CoV) (Fig. 1b). The T7 promoter sequence was added upstream of the MERS-CoV cDNA genome copy. A poly A tail of 20 nt followed by an MluI restricton site was added downstream of the genome. After linearization of the genome-containing BAC plasmid at the unique MluI site, capped infectious viral RNA was transcribed *in vitro*. In order to enhance virus rescue, genomic RNA was mixed with N gene transcript [25] and electroporated into baby hamster kidney (BHK) cells. Twenty-four hours post-electroporation, BHK cell culture supernatant was transferred to VeroB4 cells. Viral genomic RNA synthesis was monitored by real-time RT-PCR [26] and recombinant virus harvested 3 days post-infection. To determine whether rMERS-CoV had growth characteristics similar to the clinical isolate, VeroB4 cells were infected at an m.o.i. of 0.001. Wild-type and recombinant virus titres were nearly identical at 24 and 48 h p.i. (Fig. 1c).

High-throughput screening of antiviral inhibitors would be greatly facilitated by using a MERS-CoV reporter virus. Scobey *et al.* described a recombinant MERS-CoV expressing RFP rather than ORF5 [27]. However, removal of ORF5 eliminates a viral protein and the generated reporter virus replicated less efficiently than the recombinant wild-type virus. In order to maintain the natural viral protein repertoire, GFP was released from a fusion protein by interruption of translation conferred by a porcine teschovirus 2A peptide sequence [28]. This sequence prevents the ribosome from forming a peptide bond. Translation is continued, but two peptide chains are generated. In order to account for the potential influence of an additional sequence on genome structure and regulatory elements, two candidate sites for GFP insertion were chosen (Fig. 2a). The first site was the 5′-end of ORF4 (rMERS-CoV-O4-GFP), whose transcription-regulatory sequence (TRS) presumably ends in front of the start codon and should thus allow insertion of foreign sequence elements without affecting regulation of transcription. The second insertion site was the 3′-end of ORF5 (rMERS-CoV-O5-GFP). The ORF5 stop codon is located well upstream of the body TRS of the ensuing envelope (E) gene, leaving a non-coding sequence of 58 nt. Insertion of an additional gene immediately upstream of the ORF5 stop codon might not cause important changes in the sequence context upstream of the E gene that is considered relevant for transcription [29].

Two-step Red-mediated recombination [24] was used to insert GFP into the full-length MERS-CoV clone at the described genome positions. This system combines homologous recombination using the Red system of bacteriophage λ with cleavage by homing endonuclease I-SceI to produce seamless insertions in target genes by recombination. The reporter viruses rMERS-CoV-O4-GFP and rMERS-CoV-O5-GFP were rescued from cDNA. Generated stocks were quantified by plaque titration revealing that rMERS-CoV-O4-GFP produced significantly smaller plaques than rMERS-CoV (average diameters 1.0 and 2.2 mm, respectively; *t*-test, $P<0.0001$), while rMERS-CoV-O5-GFP produced even smaller and more heterogeneous plaques than rMERS-CoV (average diameter 0.7 mm; *t*-test, $P<0.0001$, Fig. 2b). Growth of the reporter viruses was compared to that of rMERS-CoV. VeroB4 cells were infected with the three recombinant viruses at an m.o.i. of 0.001 and supernatants titred at 24 and 48 h p.i. Both reporter viruses reached slightly lower titres compared to rMERS-CoV, with growth pattern rMERS-CoV>rMERS-CoV-O4-GFP>rMERS-CoV-O5-GFP (Fig. 2c). Immunofluorescence microscopy showed GFP expression in cells infected with both types of reporter virus, but not in cells infected with rMERS-CoV (Fig. 2d).

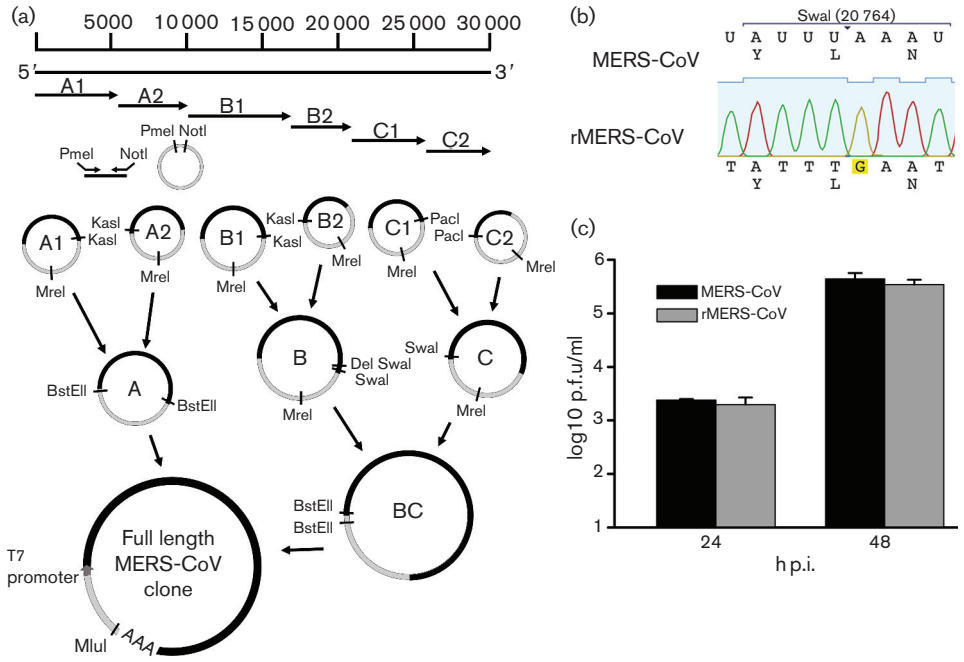

Fig. 1. MERS-CoV reverse genetics system. Overview of the MERS-CoV reverse genetics system cloning strategy (a). Six subgenomic fragments of the MERS-CoV genome were cloned into low-copy BAC vector using PmeI and NotI. Naturally occurring restriction sites were subsequently used to assemble the full-length genome. An SwaI restriction site was deleted and served as a marker mutation (b). Infection of VeroB4 cells with wild-type (MERS-CoV) and recombinant virus (rMERS-CoV) at an m.o.i of 0.001 revealed identical growth dynamics for both viruses (c).

The intensity of fluorescence was significantly higher in rMERS-CoV-O4-GFP-infected cells compared to rMERS-CoV-O5-GFP-infected cells (*t*-test, $P<0.0001$, Fig. 2e).

Because of its more efficient growth, only rMERS-CoV-O4-GFP was included in further experiments. A Western blot analysis confirmed that rMERS-CoV- and rMERS-CoV-O4-GFP-infected cells expressed similar amounts of ORF4a-encoded p4a, but only cells infected with the reporter virus expressed GFP (Fig. 3a). Interruption of translation mediated by the 2A peptide was verified by the absence of detectable GFP-p4a fusion protein. To correlate the production of infectious particles against the expression of the fluorescence marker, VeroB4 cells were infected with rMERS-CoV-O4-GFP. Cell culture supernatants were titred and the fluorescence intensity measured quantitatively at various time points. At 48 h p.i., infectious virus titres and fluorescence reached maximum values (Fig. 3b). Fluorescence signal declined subsequently, with infectious viral titres remaining at plateau level. Cells infected with rMERS-CoV showed virus production but no fluorescence signal in the quantitative readout.

The reporter virus rMERS-CoV-O4-GFP was assessed for its suitability in viral inhibitor testing using the CoV inhibitor cyclosporin A (CsA) [23, 30]. The spectrum of activity of CsA is known to include MERS-CoV [31]. VeroB4 cells were infected with rMERS-CoV-O4-GFP at an m.o.i. of 0.1, and cultivated in the presence of CsA at concentrations between 1 and 16 µM for 48 h. Virus growth (in percentage) was plotted against the logarithmic CsA concentrations (Fig. 4a). IC_{50} was calculated to be 2.41 µM. At this concentration cell viability was still 100 %. Potential differences in CsA activity against rMERS-CoV and rMERS-CoV-O4-GFP were determined by virus titration. IC_{50} values for rMERS-CoV and rMERS-CoV-O4-GFP were 5.92 and 4.62 µM, respectively, differing by a factor of 1.3 (Fig. 4b).

DISCUSSION

Here we present a novel MERS-CoV reverse genetics system that combines the advantages of existing systems for CoV reverse genetics. It uses a BAC-maintained cDNA full-length genome [32] that does not require *in vitro* ligation of fragments before RNA transcription [27]. This approach may improve the reliability of viral genome cDNA recovery. Second, it uses *in vitro* transcribed RNA to initiate replication in transfected cells, obviating the need for the viral cDNA genome to be transcribed in the nucleus, where it may undergo unwanted splicing [32]. Recombination-based mutagenesis was more rapid than classical mutagenesis because it circumvents the introduction of mutations at the level of subclones, necessary in classical mutagenesis [23]. Recombination-based mutagenesis moreover yielded a higher frequency of mutated clones due to the use of an additional positive selection marker.

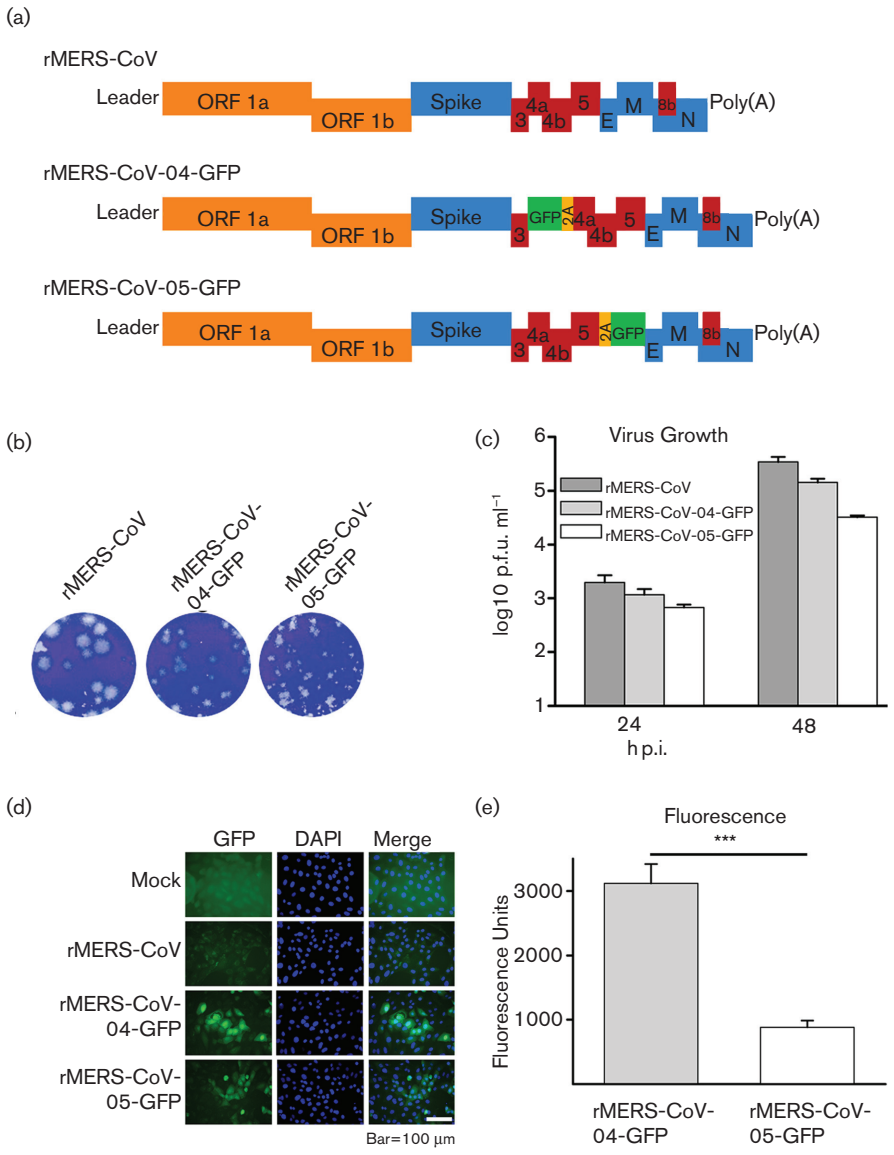

Fig. 2. Comparison of different rMERS-CoV reporter viruses. Two different reporter viruses were generated. GFP was linked via a 2A peptide to either open reading frame (ORF) 4a or 5 (a). Plaque phenotypes of reporter viruses were compared to rMERS-CoV (b). VeroB4 cells were infected with rMERS-CoV or the reporter viruses at an m.o.i. of 0.001. Supernatants were plaque-titred at indicated time points (c). In order to verify GFP expression, VeroB4 cells were infected at an m.o.i. of 0.1 and fixed 48 h later. Nuclei were stained with DAPI (d). Comparative quantification of fluorescence signals was done at 48 h post-infection of VeroB4 at m.o.i. 0.1 with both reporter viruses (e).

The genomic insertion site of reporter genes is critical. The reporter can be fused to a viral gene or replace a viral gene. The advantage of the first option is that no viral gene is lost that would be critically needed for replication or interaction with the host cell. Nevertheless, the genetic modification may also affect the function and/or expression of the protein. Insertion of the reporter gene rather than a non-essential, accessory gene might minimize the impact on reporter virus replication in cell culture [33, 34]. The previously published reporter-expressing rMERS-CoV has its accessory gene ORF5 replaced by RFP [27]. However, p5 inhibits the induction of IFN-β production by preventing nuclear translocation of IFN regulatory factor 3 [22]. In a growth analysis this virus yielded 10-fold lower virus yield compared to the parental virus in an immortalized cell line. In primary alveolar type II pneumocytes, primary lung microvascular endothelial cells and primary lung fibroblasts, the reporter virus yielded between 10- and 100-fold less progeny [22]. Although some loss of replication level can be tolerated in many experimental settings, we favoured a less invasive reporter expression strategy based on insertion of a picornavirus 2A peptide. This sequence of 22 amino acids

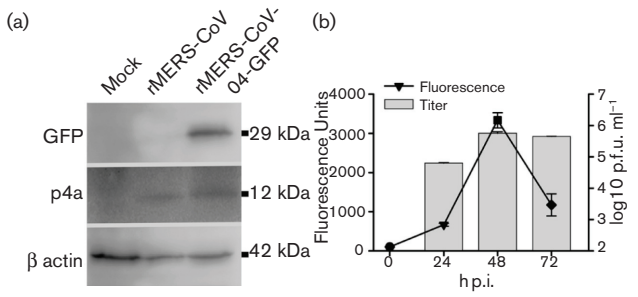

Fig. 3. Assessment of rMERS-CoV-O4-GFP reporter virus. (a) VeroB4 cells were either mock infected or infected with rMERS-CoV or rMERS-CoV-O4-GFP at m.o.i. 1 for 48 h. Expression of p4a and GFP was confirmed by Western blot analysis using rabbit anti-p4a Ig (1 : 1250, Eurogentec) and rabbit anti-GFP Ig (1 : 2000, Life Technologies). Detection of β-actin (mouse anti-β-actin, 1 : 5000, Sigma Aldrich) served as loading control. (b) After infection of VeroB4 cells at m.o.i. 0.1, samples were taken at designated time points. Supernatants were plaque-titreed and cells analysed for fluorescence.

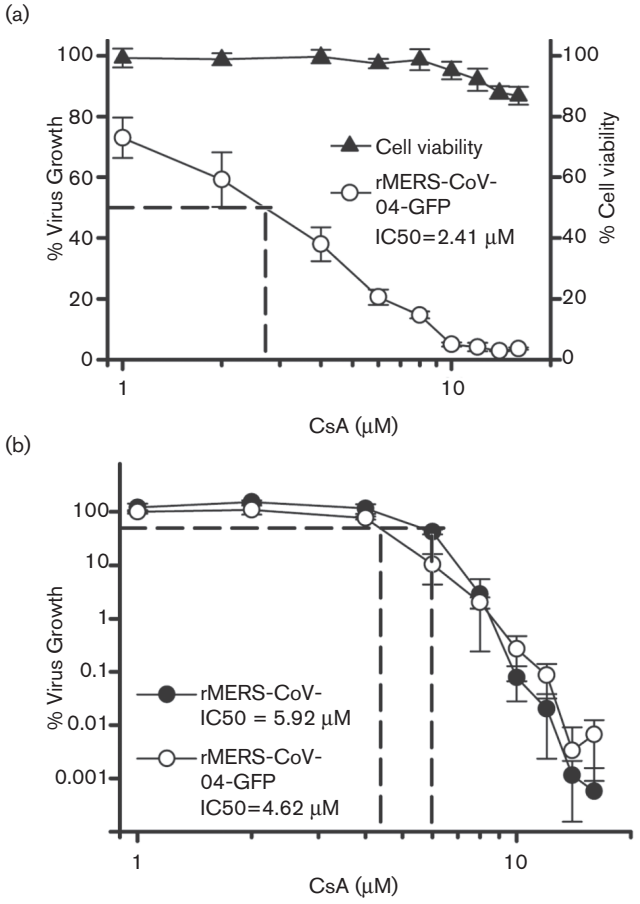

Fig. 4. Quantification of rMERS-CoV growth inhibition by CsA. VeroB4 cells were seeded in 96-well plates and infected with recombinant virus at m.o.i. 0.1 for 48 h. (a) The fluorescence signals of rMERS-CoV-O4-GFP were used to calculate virus growth (in %). Cell viability was determined in non-infected but otherwise equally treated cells. (b) Cell culture supernatants were plaque-titred for determination of virus growth (in %).

from porcine teschovirus facilitates autonomous and highly efficient intra-ribosomal self-processing of polyproteins [28, 35]. The viral gene to which the reporter gene is fused will be left unaffected by this strategy, as previously demonstrated for other plus-strand RNA viruses such as dengue-, Sindbis- and Seneca Valley virus [36–38].

The coronaviral genome is sensitive to alterations. Mutations can influence the transcription level if located in core TRS elements, in the upstream (5′-proximal) TRS context, as well as in distant genome regions [39, 40]. In this study, two alternative sites were chosen for the insertion of GFP to account for proximal sequence interactions. The first insertion site chosen was the 5′-end of ORF4a. Excepting the ORF4a start codon, all other parts of the TRS are located upstream of ORF4a. At the alternative insertion site in the 3′-part of ORF5, the ensuing E gene starts 58 nt downstream of the termination codon, preserving much of the upstream context of the E-gene TRS. The observed loss of growth efficiency associated with this insertion site may be due to long-distance RNA-RNA interactions [39]. For instance, it has been described for transmissible gastroenteritis virus that secondary structures within 600 nt upstream of the nucleocapsid gene's core TRS are necessary for optimal transcription. CoVs lacking the E gene are replication-incompetent or severely attenuated [41, 42]. However, as we have not focused on the ORF5-GFP construct for establishing the reporter virus, we have not tested p5 and E expression.

rMERS-CoV-O4-GFP replicated to viral titres comparable to rMERS-CoV and showed wild type-like expression of p4a. The selected insertion site at the 5′-end of ORF4a thus allowed seamless integration of GFP and is most likely to be useful for integration of other foreign genes into the MERS-CoV genome. No GFP-p4a fusion protein was detected by Western blot analysis, proving the highly efficient activity of the 2A peptide. An observation of practical importance was that the fluorescence signal of rMERS-CoV-O4-GFP was highest at 48 h p. i. and declined afterwards, while the level of viral particles in the cell culture supernatant remained constant. GFP may be degraded during apoptotic or normal cell metabolism, whereas viral particles accumulate outside cells and remain infectious for a considerable time in the supernatant. GFP readout for the antiviral inhibitor test was therefore done at 48 h p.i.

When testing the known MERS-CoV inhibitor CsA, the IC_{50} based on fluorescence signal was in the same range as that using infectious particles and corresponded to the effective CsA concentration identified in a previous study [31]. The IC_{50} values determined using rMERS-CoV-O4-GFP versus rMERS-CoV differed by a factor of 1.3 only. This is most likely an intra-assay variation, but we cannot exclude causation by a slightly impaired growth of the reporter

virus, requiring reduced CsA concentrations for efficient growth inhibition.

In summary, we describe a new reverse genetics system for MERS-CoV that can be mutated easily and time-efficiently by homologue recombination. Based on this system we identified a suitable genome position for the insertion of a reporter gene without losing expression of viral proteins.

METHODS

General cell culture conditions

VeroB4 (DSMZ-AC33) and BHK cells (CCL-10) were maintained in Dulbecco's modified Eagle's medium (DMEM) supplemented with 10 % fetal bovine serum, 1 % penicillin/streptomycin, 1 % non-essential amino acids, 1 % L-glutamine and 1 % sodium pyruvate (all Thermo Fisher Scientific) in a 5 % CO_2 atmosphere at 37 °C.

Virus growth kinetics and plaque titration

Twenty-four hours prior to infection, Vero B4 cells were seeded in 6-well plates at a concentration of 2×10^5 cells ml^{-1}. The supernatant was removed and cells washed once with PBS (Thermo Fisher Scientific) before virus (diluted in OptiPro serum-free medium, Thermo Fisher Scientific) adsorption. After incubation for 1 h, virus-containing supernatant was removed, and cells washed twice with PBS and supplied with DMEM as described above. Plaque titration was done as described elsewhere [23, 43]. Briefly, 1×10^5 VeroB4 cells were seeded per well in a 24-well plate 24 h prior to infection with a serial dilution of virus-containing cell culture supernatant diluted in OptiPro. One hour after adsorption, supernatants were discarded and cells overlaid with 2.4 % Avicel (FMC BioPolymers, Brussels, Belgium) diluted 1 : 2 in 2× DMEM supplemented with 20 % fetal bovine serum, 2 % penicillin/streptomycin, 2 % non-essential amino acids, 2 % L-glutamine and 2% sodium pyruvate. Four days post-infection the overlay was removed, and cells were fixed in 6 % formaldehyde and stained with a 0.2 % crystal violet, 2 % ethanol and 10 % formaldehyde solution. All infection experiments were done under biosafety level 3 conditions with enhanced respiratory personal protection equipment.

Construction of a MERS-CoV full-length cDNA clone

The cloning strategy was based on the genome of reference strain MERS-CoV/EMC2012 (NC_019843). The genome was divided into six subgenomic fragments of similar length (A1, A2, B1, B2, C1, C2). Isolated viral RNA was reverse transcribed using SuperScript III Reverse Transcriptase (Invitrogen) with sequence-specific primers. Primers used in cDNA synthesis were 5′-cttgcacttccagtctgaagtc-3′, 5′-catcataattaggatcagacaactg-3′, 5′-tacggtgagttaaggtacttctg-3′ and 5′-ttttttttttttttttttttgcaaatcatctaattagcc-3′ for fragments A1, A2, C1 and C2, respectively. PCR was done with Phusion High-Fidelity DNA Polymerase (NEB) or Expand High Fidelity PCR System (Roche). Fragments A1 and A2 were amplified using primers A1-for 5′-*agctttt*GTTTAAAC taatacgactcactatagg*atttaagtgaatagcttggctatc*-3′ and A1-rev A5′-*atagtttta*GCGGCCGCatggccaacagccgtttcaatg-3′ and A2-for 5′-*agctttt*GTTTAAACggttgctgctctcaggcac-3′ and A2-rev 5′-*atagtttta*GCGGCCGCcaagccaaagaccattaagagtc-3′. Fragments C1 and C2 were amplified with primers C1-for 5′-*agctttt*GTTTAAACtggggttatgtaggcaatcttg-.3′ and C1-rev 5′-*atagtttta*GCGGCCGCagcagagacacgtaatccatag-3′ and C2-for 5′-*agctttt*GTTTAAACgtgaatctttttgacgttggttac-3′ and C2-rev 5′-*ataagaat*GCGGCCGC**acgcgt**ttttttttttttttttttttttgcaaatcatcta attagcc-3′. The underlined sequence in primer A1-for represents the minimal T7 promoter sequence. Capital letters represent restriction sites PmeI in forward and NotI in reverse primers. Italic sequences denote additional nts for optimal performance of restriction enzymes. Fragments were cloned into bacterial artificial chromosome vectors (pBeloBAC 11, modified as described in Pfefferle *et al.* [23] and additionally modified to carry an Sse232I restriction site in the repA gene, substitution T306C) using restriction sites PmeI and NotI introduced via PCR primers. A 20 nt poly (T) tail and an MluI restriction site (bold in primer C2-rev) were added to the 3' end of fragment C2 via primers.

Fragments B1 and B2 were synthetically generated (GeneArt, Thermo Fisher Scientific) due to insert instability during cloning. B1 comprised genome positions 10 076–16 920 (BstEII – KasI) and B2 comprised genome positions 16 915–20 905 (KasI–SwaI). The natural SwaI restriction site at genome position 20 764 was deleted during synthesis (ATTTAAAT→ATTgAAT), thus preserving the amino acid sequence.

All cloned fragments were Sanger sequenced whereupon non-silent mutations in fragments A1, A2 and C2 were noted when compared to the Genbank entry. All three fragments were corrected using the Phusion Site-Directed Mutagenesis Kit (Thermo Fisher Scientific) and again Sanger sequenced. Fragment A1 was corrected using primers 5′-CGTTGATCTTTCAGTAGCT**T**CTACCTATTTT TTAGTCC-3′ and 5′-CAATCAAAAAGTAGTTCACTA AAGGATGACACACCAG-3′. Fragment A2 was corrected using primers 5′-GCAGGTACATTGCATTA**T**TTCTTT GCACAGACTTC-3′ and 5′-CAACAACAACCAGTTGA AGGCCGAGGTATAG-3′. Fragment C2 was corrected using primers 5′-TTATCCTCATAATACTTT**G**GTTTG TAGATAGAATTCGTTTC-3′ and 5′-CTAAGAAGGCTA TCAGGCAACTTCCAGTTGG-3′. Depicted in bold and underlined are the corrected nts. The mutation in fragment C2 was a premature stop codon (TAG) within ORF5, which is present in the viral isolate.

All plasmids were digested at the naturally occurring restriction sites indicated, digested plasmids separated on a 0.8 % agarose gel and desired fragments purified using NucleoSpin Gel and PCR Clean-up (Macherey-Nagel) or QIAEXX II Gel Extraction Kits (QIAGEN). Ligation was performed for 16 h at 14 °C using T4 DNA Ligase (Roche). The full-length genome-containing plasmid was Sanger sequenced. The integrity of the genomic and sub-genomic inserts was checked using PCRs that amplify the whole insert in

overlapping fragments of 3–4 kb prior to downstream applications.

Rescue of recombinant MERS-CoV

Rescue of recombinant virus was carried out as already described for SARS-CoV [23]. Genomic viral RNA was transcribed *in vitro* from 1 µg MluI linearized and phenol-chloroform extracted full-length plasmid using Ambion's mMESSAGE mMACHINE Kit. Additionally, capped nucleocapsid transcript was generated using 1 µg of a purified PCR product spanning the N gene (forward primer adding SP6 promoter sequence: 5′-ggccatttaggtgacactatagatggcatcccctgctgcac-3′, reverse primer: 5′- ttttttttttttttttttttgcaaatcatctaattagcc-3′). Ten µg of genomic viral RNA and 2 µg of N gene transcript were added to 4×10^6 BHK cells resuspended in 100 µl OptiPro and electroporated in a 2 mm gap cuvette by applying one pulse of 140 V in 25 msec in a Gene Pulser Xcell (Biorad). Electroporated cells were grown for 24 h in a T75 cell culture flask. Cell culture supernatant was then transferred to susceptible VeroB4 cells and viral genomic RNA synthesis monitored for 3 days by real-time RT-PCR [26] before progeny virus was harvested, plaque titred and stocked for further use.

Generation of MERS-CoV reporter viruses by Red-mediated recombination

Red-mediated recombination was done as previously described [24]. The molecular procedure is shown in Fig. 5 using the insertion of the GFP at the 5′-end of ORF4a as an example. The full-length cDNA plasmid was transformed into *E. coli* strain GS1783. This strain carries chromosomally encoded genes for Red recombination under a temperature-inducible promoter and the *I-sceI* gene under an arabinose-inducible promoter. The Porcine teschovirus 2A peptide was cloned to the N- and C-terminus of the GFP gene (cDNA for codon-optimized *Aequorea coerulescens* GFP was kindly provided by Dr Sebastian Hauka, Institute of Virology, University of Bonn Medical Centre). The universal transfer construct was created by inserting a selection marker cassette, consisting of an I-SceI restriction site, a kanamycin resistance gene and a short-sequence duplication (50 nts) of GFP into the GFP sequence using the unique restriction site AgeI. The universal transfer construct was PCR amplified using specific primers that contained 5′-extensions of approx. 50 nts, corresponding to the MERS-CoV sequence at the site of recombination. PCR primers MERS-GFP-4-F (5′-agtgtgaatctttttgacgttggttactcagttaattaacgaactctatggtgtctaaaggagccgagctg-3′) and MERS-GFP-4-R (5′-ggtgagttaaggtacttctgccaaatttgattaagcagagacacgtaatccatag gtccagggttctcctccac-3′) were used for the insertion of GFP at the 5′-end of ORF4a. Primers MERS-GFP-5-F (5′-cgcgcgatt-cagttcctcttcacataatcgccccgagctcgcttatcgttggaagcggagctactaac ttc-3′) and MERS-GFP-5-R (5′-actaatggattagcctctacacg ggacccatagtagcgcagagctgcttaatacagttcgtccatgccgtg-3′) were used for the insertion of GFP at the 3′-end of ORF5. The PCR product was DpnI digested and gel purified to reduce input plasmid contamination. The purified PCR product was electroporated into *E.coli* strain GS1783 containing the full-length MERS-CoV BAC clone and recombination was initiated. Selection of positive clones was done on LB-agar plates containing 30 µg ml^{-1} chloramphenicol and 30 µg ml^{-1} kanamycin at 32 °C for 48 h. Positive clones were screened by a PCR spanning the recombination site. To remove the kanamycin resistance cassette, *in vivo* cleavage was induced at the I-SceI site using 1 % L-(+) arabinose. A second recombination was induced by incubation of *E. coli* GS1783 at 42 °C for 30 min. Positive clones were selected on LB-agar plates containing 1 % L-(+) arabinose and 30 µg ml^{-1} chloramphenicol. Successful recombination resulting in a full-length MERS-CoV cDNA genome carrying the GFP gene was confirmed by sequencing of recombination sites and the insert.

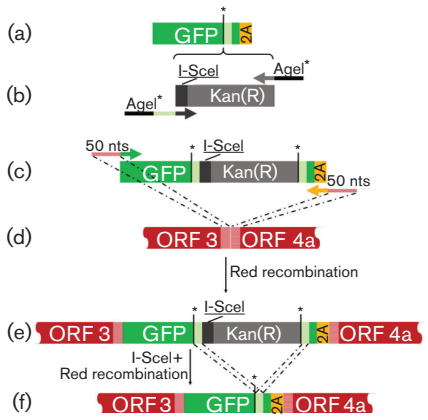

Fig. 5. Procedure of Red-mediated mutagenesis. Insertion of GFP at the 5′-end of MERS-CoV ORF4a is exemplified. A unique restriction site was chosen (a) where the marker cassette was inserted (b). This universal transfer construct was PCR amplified (c), and 50 nt corresponding to the site of recombination (d) were added. During the first Red recombination, GFP and the marker cassette were inserted at the 5′-end of ORF4a (e). The marker cassette was then excised by *in vivo* cleavage at the I-SceI site and a second Red recombination (f). Adapted from [24].

Immunofluorescence

Vero B4 cells were seeded at a density of 5×10^4 cells ml^{-1} in a 24-well plate containing glass slides 24 h before infection. Cells were mock-infected or infected with rMERS-CoV, rMERS-CoV-O4-GFP or rMERS-CoV-O5-GFP at an m.o.i. of 0.1. Forty-eight hours post-infection, cells were washed twice with PBS and fixed with 6 % formaldehyde for 1 h. Cells were washed twice with PBS and glass slides were mounted using ProLong Gold Antifade mounting medium containing DAPI (Thermo Fisher Scientific). Slides were left to dry in the dark and stored at 4 °C until fluorescence microscopy was performed.

Western blot

Vero B4 cells (3.5×10^5 cells ml^{-1}) were seeded in 6-well plates 24 h prior to mock infection or infection with rMERS-CoV or rMERS-CoV-O4-GFP at an m.o.i. of 1.

Forty-eight hours post-infection, cells were washed once with ice-cold PBS, scraped into 1 ml PBS and centrifuged for 10 min at 300 ***g*** and 4 °C. Cell pellets were lysed in 50 µl Pierce IP Lysis Buffer (Thermo Fisher Scientific) supplied with 100× Protease Inhibitor Cocktail Set III (Merck Millipore) for 30 min at 4 °C. Cell debris was pelleted for 10 min at 13 000×g and 4 °C and the supernatant transferred to a fresh tube and mixed with 4× NuPAGE LDS Sample Buffer (Thermo Fisher Scientific) supplied with 10 % 2-mercaptoethanol (Roth). Samples were inactivated for 10 min at 99 °C. Proteins were separated on a 12 % sodium dodecyl sulfate-polyacrylamid gel and transferred onto a 0.2 µm PVDF membrane (Merck Millipore) by semi-dry blotting (Biometra). Detection of 12 kDa MERS-CoV p4a was done using a polyclonal rabbit anti-p4a antibody (1 : 1250, Eurogentec), a horseradish peroxidase (HRP)-coupled goat anti-rabbit antibody (1 : 10,000, Dianova) and SuperSignal West Femto Chemiluminescence Substrate (Thermo Fisher Scientific). The membrane was stripped of antibodies using ReBlot Plus Strong Antibody Stripping Solution (10×, Merck Millipore) and probed again with mouse anti-β actin (1 : 5000, Sigma Aldrich) and rabbit anti-GFP (1 : 2000, Life Technologies) antibodies. Visualization was done as described above, additionally using goat anti-mouse HRP antibody (1 : 10,000, Dianova).

Inhibitor test

Vero B4 cells were seeded at a concentration of 2×10^5 cells ml^{-1} in a black 96-well plate 24 h prior to infection. Cells were infected with rMERS-CoV or rMERS-CoV-O4-GFP at an m.o.i. of 0.1 as described above. After 1 h of virus adsorption the inoculum was removed, and DMEM without phenol red containing 10 % FCS and different concentrations of cyclosporine A (1–16 µM) was applied. Fluorescence intensity was measured 48 h post-infection, for which infection medium was removed, cells washed once with PBS and 50 µl of PBS applied to each well. Fluorescence readout was performed without the plate lid using a Synergy Mx microplate reader (Biotek) at the following settings: excitation (gap): 475 nm (13.5); emission (gap): 505 nm (13.5); gain: 100 V; readings per well: 30; read height: 4.5 mm; temperature: 37 °C. Titration of supernatants was performed as described above. Cytotoxicity of CsA was determined using the CellTiter-Glo Luminescent Cell Viability Assay (Promega). Vero B4 cells were seeded exactly as described above and treated with the same concentrations of CsA that were used for the inhibitor assay. After 48 h, 50 µl of medium was replaced by 50 µl of CellTiter-Glo substrate and incubated for 10 min. Luminescence was read according to the manufacturer's instructions. In order to calculate the percentage of virus growth or cell viability, fluorescence or luminescence signals determined at 0 µM CsA were set to 100 %.

Funding information
This work was funded by the German Research Foundation through project number DR 772/12-1.

Acknowledgements
We thank Ron Fouchier (Erasmus University, Rotterdam) for providing MERS-CoV strain EMC2012. We are grateful to Artem Siemens for excellent technical assistance.

Conflicts of interest
The authors declare that there are no conflicts of interest.

References

1. **Sweileh WM.** Global research trends of World Health Organization's top eight emerging pathogens. *Global Health* 2017;13:9.
2. **World Health Organization.** www.who.int/emergencies/mers-cov/en/ [accessed 24 April 2017].
3. **Bermingham A, Chand MA, Brown CS, Aarons E, Tong C *et al.*** Severe respiratory illness caused by a novel coronavirus, in a patient transferred to the United Kingdom from the Middle East, September 2012. *Euro Surveill* 2012;17:20290.
4. **Wernery U, Corman VM, Wong EY, Tsang AK, Muth D *et al.*** Acute middle East respiratory syndrome coronavirus infection in livestock Dromedaries, Dubai, 2014. *Emerg Infect Dis* 2015;21:1019–1022.
5. **Alagaili AN, Briese T, Mishra N, Kapoor V, Sameroff SC *et al.*** Middle East respiratory syndrome coronavirus infection in dromedary camels in Saudi Arabia. *MBio* 2014;5:e00884-14.
6. **Farag EA, Reusken CB, Haagmans BL, Mohran KA, Stalin Raj V, Raj S V *et al.*** High proportion of MERS-CoV shedding dromedaries at slaughterhouse with a potential epidemiological link to human cases, Qatar 2014. *Infect Ecol Epidemiol* 2015;5:28305.
7. **Corman VM, Jores J, Meyer B, Younan M, Liljander A *et al.*** Antibodies against MERS coronavirus in dromedary camels, Kenya, 1992-2013. *Emerg Infect Dis* 2014;20:1319–1322.
8. **Müller MA, Corman VM, Jores J, Meyer B, Younan M *et al.*** MERS coronavirus neutralizing antibodies in camels, Eastern Africa, 1983–1997. *Emerg Infect Dis* 2014;20:2093–2095.
9. **Breban R, Riou J, Fontanet A.** Interhuman transmissibility of Middle East respiratory syndrome coronavirus: estimation of pandemic risk. *Lancet* 2013;382:694–699.
10. **Chowell G, Abdirizak F, Lee S, Lee J, Jung E *et al.*** Transmission characteristics of MERS and SARS in the healthcare setting: a comparative study. *BMC Med* 2015;13:210.
11. **Drosten C, Meyer B, Müller MA, Corman VM, Al-Masri M *et al.*** Transmission of MERS-coronavirus in household contacts. *N Engl J Med* 2014;371:828–835.
12. **Korea Centers for Disease Control and Prevention.** Middle East respiratory syndrome coronavirus outbreak in the Republic of Korea, 2015. *Osong Public Health Res Perspect* 2015;6:269–278.
13. **Assiri A, McGeer A, Perl TM, Price CS, Al Rabeeah AA *et al.*** Hospital outbreak of Middle East respiratory syndrome coronavirus. *N Engl J Med* 2013;369:407–416.
14. **Oboho IK, Tomczyk SM, Al-Asmari AM, Banjar AA, Al-Mugti H *et al.*** 2014 MERS-CoV outbreak in Jeddah-a link to health care facilities. *N Engl J Med* 2015;372:846–854.
15. **Mo Y, Fisher D.** A review of treatment modalities for Middle East respiratory syndrome. *J Antimicrob Chemother* 2016;71:3340–3350.
16. **Perlman S, Vijay R.** Middle East respiratory syndrome vaccines. *Int J Infect Dis* 2016;47:23–28.
17. **Niemeyer D, Zillinger T, Muth D, Zielecki F, Horvath G *et al.*** Middle East respiratory syndrome coronavirus accessory protein 4a is a type I interferon antagonist. *J Virol* 2013;87:12489–12495.
18. **Rabouw HH, Langereis MA, Knaap RCM, Dalebout TJ, Canton J *et al.*** Middle East Respiratory coronavirus accessory protein 4a inhibits PKR-mediated antiviral stress responses. *PLoS Pathog* 2016;12:e1005982.
19. **Thornbrough JM, Jha BK, Yount B, Goldstein SA, Li Y *et al.*** Middle East respiratory syndrome coronavirus NS4b protein inhibits host rnase l activation. *MBio* 2016;7:e00258.

20. Matthews KL, Coleman CM, van der Meer Y, Snijder EJ, Frieman MB. The ORF4b-encoded accessory proteins of Middle East respiratory syndrome coronavirus and two related bat coronaviruses localize to the nucleus and inhibit innate immune signalling. *J Gen Virol* 2014;95:874–882.
21. Yang Y, Ye F, Zhu N, Wang W, Deng Y *et al.* Middle East respiratory syndrome coronavirus ORF4b protein inhibits type I interferon production through both cytoplasmic and nuclear targets. *Sci Rep* 2015;5:17554.
22. Yang Y, Zhang L, Geng H, Deng Y, Huang B *et al.* The structural and accessory proteins M, ORF 4a, ORF 4b, and ORF 5 of Middle East respiratory syndrome coronavirus (MERS-CoV) are potent interferon antagonists. *Protein Cell* 2013;4:951–961.
23. Pfefferle S, Krähling V, Ditt V, Grywna K, Mühlberger E *et al.* Reverse genetic characterization of the natural genomic deletion in SARS-Coronavirus strain Frankfurt-1 open reading frame 7b reveals an attenuating function of the 7b protein *in vitro* and *in vivo*. *Virol J* 2009;6:131.
24. Tischer BK, von Einem J, Kaufer B, Osterrieder N. Two-step red-mediated recombination for versatile high-efficiency markerless DNA manipulation in *Escherichia coli*. *BioTechniques* 2006;40:191–197.
25. Yount B, Curtis KM, Fritz EA, Hensley LE, Jahrling PB *et al.* Reverse genetics with a full-length infectious cDNA of severe acute respiratory syndrome coronavirus. *Proc Natl Acad Sci USA* 2003;100:12995–13000.
26. Corman VM, Eckerle I, Bleicker T, Zaki A, Landt O *et al.* Detection of a novel human coronavirus by real-time reverse-transcription polymerase chain reaction. *Euro Surveill* 2012;17:pii=20285.
27. Scobey T, Yount BL, Sims AC, Donaldson EF, Agnihothram SS *et al.* Reverse genetics with a full-length infectious cDNA of the Middle East respiratory syndrome coronavirus. *Proc Natl Acad Sci USA* 2013;110:16157–16162.
28. de Felipe P. Skipping the co-expression problem: the new 2A "CHYSEL" technology. *Genet Vaccines Ther* 2004;2:13.
29. Van Boheemen S, de Graaf M, Lauber C, Bestebroer TM, Raj VS *et al.* Genomic characterization of a newly discovered coronavirus associated with acute respiratory distress syndrome in humans. *MBio* 2012;3:e00473-12.
30. Pfefferle S, Schöpf J, Kögl M, Friedel CC, Müller MA *et al.* The SARS-coronavirus-host interactome: identification of cyclophilins as target for pan-coronavirus inhibitors. *PLoS Pathog* 2011;7:e1002331.
31. de Wilde AH, Raj VS, Oudshoorn D, Bestebroer TM, van Nieuwkoop S *et al.* MERS-coronavirus replication induces severe *in vitro* cytopathology and is strongly inhibited by cyclosporin A or interferon-α treatment. *J Gen Virol* 2013;94:1749–1760.
32. Almazán F, Dediego ML, Sola I, Zuñiga S, Nieto-Torres JL *et al.* Engineering a replication-competent, propagation-defective Middle East respiratory syndrome coronavirus as a vaccine candidate. *MBio* 2013;4:e00650-13.
33. Weiss SR, Leibowitz JL. Coronavirus pathogenesis. *Adv Virus Res* 2011;81:85–164.
34. Weiss SR, Navas-Martin S. Coronavirus pathogenesis and the emerging pathogen severe acute respiratory syndrome coronavirus. *Microbiol Mol Biol Rev* 2005;69:635–664.
35. Kim JH, Lee SR, Li LH, Park HJ, Park JH *et al.* High cleavage efficiency of a 2A peptide derived from porcine teschovirus-1 in human cell lines, zebrafish and mice. *PLoS One* 2011;6:e18556.
36. Leardkamolkarn V, Sirigulpanit W. Establishment of a stable cell line coexpressing dengue virus-2 and green fluorescent protein for screening of antiviral compounds. *J Biomol Screen* 2012;17:283–292.
37. Poirier JT, Reddy PS, Idamakanti N, Li SS, Stump KL *et al.* Characterization of a full-length infectious cDNA clone and a GFP reporter derivative of the oncolytic picornavirus SVV-001. *J Gen Virol* 2012;93:2606–2613.
38. Thomas JM, Klimstra WB, Ryman KD, Heidner HW. Sindbis virus vectors designed to express a foreign protein as a cleavable component of the viral structural polyprotein. *J Virol* 2003;77:5598–5606.
39. Mateos-Gomez PA, Morales L, Zuñiga S, Enjuanes L, Sola I. Long-distance RNA-RNA interactions in the coronavirus genome form high-order structures promoting discontinuous RNA synthesis during transcription. *J Virol* 2013;87:177–186.
40. Sola I, Moreno JL, Zúñiga S, Alonso S, Enjuanes L. Role of nucleotides immediately flanking the transcription-regulating sequence core in coronavirus subgenomic mRNA synthesis. *J Virol* 2005;79:2506–2516.
41. Dediego ML, Alvarez E, Almazán F, Rejas MT, Lamirande E *et al.* A severe acute respiratory syndrome coronavirus that lacks the E gene is attenuated *in vitro* and *in vivo*. *J Virol* 2007;81:1701–1713.
42. Ortego J, Ceriani JE, Patiño C, Plana J, Enjuanes L. Absence of E protein arrests transmissible gastroenteritis coronavirus maturation in the secretory pathway. *Virology* 2007;368:296–308.
43. Matrosovich M, Matrosovich T, Garten W, Klenk H-D. New low-viscosity overlay medium for viral plaque assays. *Virol J* 2006;3:63.